

Symplectic Integrators in Corotating Coordinates

Xiongbiao Tu¹, Qiao Wang^{1,4}, Yifa Tang^{2,3}

¹National Astronomical Observatories, Chinese Academy of Sciences, Beijing 100101, China

²LSEC, ICMSEC, Academy of Mathematics and Systems Science, Chinese Academy of Sciences, Beijing 100190, China

³School of Mathematical Sciences, University of Chinese Academy of Sciences, Beijing 100049, China

⁴School of Astronomy and Space Science, University of Chinese Academy of Sciences, Beijing 100049, China
qwang@nao.cas.cn Received 0000 xxxx 00; accepted 0000 xxxx 00

Abstract The dynamic equation of mass point in rotating coordinates is governed by Coriolis and centrifugal force, besides a corotating potential relative to frame. Such a system is no longer a canonical Hamiltonian system so that the construction of symplectic integrator is problematic. In this paper, we present three integrators for this question. It is significant that those schemes have the good property of near-conservation of energy. We proved that the discrete symplectic map of $(\mathbf{p}_n, \mathbf{x}_n) \mapsto (\mathbf{p}_{n+1}, \mathbf{x}_{n+1})$ in corotating coordinates exists and the two integrators are variational symplectic. Two groups of numerical experiments demonstrates the precision and long-term convergence of these integrators in the examples of corotating top-hat density and circular restricted three-body system.

Key words: methods: numerical – celestial mechanics

1 INTRODUCTION

Canonical Hamiltonian system could be the most important physical systems and a canonical Hamiltonian system in the variables $\mathbf{z} = (p, q)$ given in the form

$$\begin{aligned}\dot{p} &= -H_q(p, q) \\ \dot{q} &= H_p(p, q)\end{aligned}\quad (1)$$

where $p, q \in \mathbb{R}^d$. Or equivalently

$$\dot{\mathbf{z}} = J^{-1} \nabla H(\mathbf{z}), \quad J = \begin{pmatrix} 0 & I_d \\ -I_d & 0 \end{pmatrix}, \quad (2)$$

where $\mathbf{z} = (\mathbf{x}, \mathbf{v})^\top$ and I_d is a $d \times d$ identity matrix. It has an outstanding property that the flow of Hamiltonian system is symplectic. It is natural to find those discrete systems which preserve the properties of symplecticity and the inner symmetries of original Hamiltonian system. So the symmetric, symplectic algorithms (Feng 1985, 1986; Forest & Ruth 1990; Channell & Scovel 1990; Candy & Rozmus 1991) are the standard methods for such problems.

For example, the implicit midpoint scheme, which is symmetric, second-order, symplectic integrator for the canonical Hamiltonian system. The other example is the well known Boris algorithm (Boris 1970) in the

plasma dynamics, which has some good geometric properties. Generally, it is symmetric, second-order, volume-preserving (Qin et al. 2013), and is not symplectic (Ellison et al. 2015). But, in special configuration of the homogeneous magnetic field, the integrator is variational symplectic and preserve near-conservation of energy over long term evolution (Ellison et al. 2015; Hairer & Lubich 2018).

Unfortunately, the motion of mass points in corotating frame is a non-canonical Hamiltonian system. So it is not available to construct symplectic numerical methods in the direct approach. However, the calculation of precise numerical orbit is critical for the dynamic studies of binary star system, central bar in galaxies, etc (Binney & Tremaine 2008). Even considering a simple restricted three body problem, such as halo orbits about Lagrange points, it is non-trivial to find a high precise orbit in Earth-Moon corotating coordinate (Akiyama et al. 2019; Oshima & Yanao 2019). In this work, we construct and investigate three integrators for the geometric properties or conservation in corotating potentials.

This paper is organized as follows. In Sec. 2, we give a brief introduction to corotating coordinate system and three numerical methods. In Sec. 3 and 4, we analysis the long time energy behaviours for these numerical methods and show that these numerical methods have some good

geometric properties. In Sec. 5, two groups of numerical experiments were performed to check the precision and demonstrate good geometric properties. Finally, we summarize this work in Sec. 6.

2 NUMERICAL METHODS

2.1 The corotating system

The equations of motion in corotating coordinates can be written as

$$\ddot{\mathbf{x}} + 2(\Omega \times \dot{\mathbf{x}}) = -\nabla(U(\mathbf{x}) - \frac{1}{2}\omega^2 \mathbf{r}^2), \quad (3)$$

where $\mathbf{x} = (x, y, z)$ is the position, $\Omega = (0, 0, \omega)$ means the system rotates clockwise around the z axis with rotation speed ω , $U(\mathbf{x})$ is a potential energy, and $\mathbf{r} = (x, y, 0)$. It is an Euler-Lagrange equations with Lagrangian $L(\mathbf{x}, \dot{\mathbf{x}}) = \frac{1}{2}\dot{\mathbf{x}}^2 + \Omega \cdot (\mathbf{r} \times \dot{\mathbf{r}}) - (U(\mathbf{x}) - \frac{1}{2}\omega^2 \mathbf{r}^2)$, the conjugate momenta $\mathbf{p} = \partial L / \partial \dot{\mathbf{x}} = \dot{\mathbf{x}} + (-\omega y, \omega x, 0)$ (conjugate to the position variables \mathbf{x}) derived by Legendre transform. The energy $E = \frac{1}{2}\dot{\mathbf{x}}^2 + (U(\mathbf{x}) - \frac{1}{2}\omega^2 \mathbf{r}^2)$ is an invariant along the flow of the system.

We set $\varphi(\mathbf{x}) = U(\mathbf{x}) - \frac{1}{2}\omega^2 \mathbf{r}^2$ and rewrite the corotating coordinate system (3). Let $\dot{\mathbf{x}} = \mathbf{v}$, $\mathbf{z} = (\mathbf{x}, \mathbf{v})^\top$, and \mathbf{v} is the velocity of the particle. The motion equations of the particle can be expressed as

$$\begin{cases} \dot{\mathbf{x}} = \mathbf{v}, \\ \dot{\mathbf{v}} = 2\mathbf{v} \times \Omega - \nabla\varphi(\mathbf{x}). \end{cases} \quad (4)$$

Obviously, it is a non-canonical Hamiltonian system $\dot{\mathbf{z}} = K^{-1}\nabla H(\mathbf{z})$ with

$$K = \begin{pmatrix} \hat{\Omega} & -I_3 \\ I_3 & 0 \end{pmatrix}, \quad \hat{\Omega} = \begin{pmatrix} 0 & 2\omega & 0 \\ -2\omega & 0 & 0 \\ 0 & 0 & 0 \end{pmatrix}.$$

Here, K is an antisymmetric matrix with its entries being the rotation speed of the system rotated, and $H(\mathbf{z}) = \frac{1}{2}\mathbf{v}^2 + \varphi(\mathbf{x})$. The antisymmetric matrix K provides a K-symplectic structure, which is defined by

$$w_K = \frac{1}{2}d\mathbf{z}^\top \wedge K d\mathbf{z}.$$

An integrator $\psi : \mathbf{z}_n \mapsto \mathbf{z}_{n+1}$ is referred to as K-symplectic, when w_K is preserved by the flow of the integrator, i.e., $d\mathbf{z}_{n+1}^\top \wedge K d\mathbf{z}_{n+1} = d\mathbf{z}_n^\top \wedge K d\mathbf{z}_n$.

2.2 The Integrators

First, we introduce the implicit midpoint scheme ψ_m in corotating coordinates. It reads

$$\mathbf{z}_{n+1} = \mathbf{z}_n + \Delta t f\left(\frac{\mathbf{z}_n + \mathbf{z}_{n+1}}{2}\right). \quad (5)$$

ψ_m is a second-order implicitly symmetric scheme. It is well-known that it is only symplectic in canonical Hamiltonian system. Generally speaking, ψ_m should have been not symplectic in our non-canonical case. However we show ψ_m is indeed symplectic for the system (4) in the Section 4.

We take into account of Boris algorithm (Boris 1970) to discrete the system (3) as the numerical integrator ψ_b :

$$\frac{\mathbf{x}_{n+1} - 2\mathbf{x}_n + \mathbf{x}_{n-1}}{2\Omega \times \frac{\Delta t^2}{2\Delta t}} + \frac{\Delta t^2}{2\Delta t} \nabla\varphi(\mathbf{x}_n) = -\nabla\varphi(\mathbf{x}_n). \quad (6)$$

It is a second-order explicitly symmetric integrator. At the same time, we set the discrete velocity has the form of

$$\begin{aligned} \mathbf{v}_n &= \frac{\mathbf{x}_{n+1} - \mathbf{x}_n}{\Delta t} - \frac{1}{2}(\mathbf{x}_{n+1} - \mathbf{x}_n) \times \Omega \\ &\quad + \Delta t \nabla\varphi(\mathbf{x}_n), \\ \mathbf{v}_{n+1} &= \frac{\mathbf{x}_{n+1} - \mathbf{x}_n}{\Delta t} + \frac{1}{2}(\mathbf{x}_{n+1} - \mathbf{x}_n) \times \Omega. \end{aligned} \quad (7)$$

The map $(\mathbf{v}_n, \mathbf{x}_n) \mapsto (\mathbf{v}_{n+1}, \mathbf{x}_{n+1})$ is K-symplectic which will be verified in the Section 4.

Similarly, we discrete the system (3) on the velocity term by the numerical integrator ψ_v :

$$\frac{\mathbf{x}_{n+2} - 2\mathbf{x}_n + \mathbf{x}_{n-2}}{(2\Delta t)^2} + 2\Omega \times \frac{-\mathbf{x}_{n+2} + 8\mathbf{x}_{n+1} - 8\mathbf{x}_{n-1} + \mathbf{x}_{n-2}}{12\Delta t} = -\nabla\varphi(\mathbf{x}_n). \quad (8)$$

This numerical integrator ψ_v is a simple modify for ψ_b by using five points difference approximate for $\dot{\mathbf{x}}$. It is an explicitly symmetric, second-order numerical method.

In the next sections, we analysis the energy errors over long times and the geometry properties of these numerical methods.

3 ENERGY ERROR ANALYSIS

In this section, we analyse the energy deviation of the integrators ψ_b, ψ_v over very long times. Firstly, we consider ψ_b and solve the modified differential equation whose solution $\mathbf{y}(t)$ formally satisfies $\mathbf{y}(n\Delta t) = \mathbf{x}_n$. Thus, $\mathbf{y}(t)$ must satisfies Eq. (6), i.e.,

$$\frac{\mathbf{y}(t + \Delta t) - 2\mathbf{y}(t) + \mathbf{y}(t - \Delta t)}{2\Omega \times \frac{\Delta t^2}{2\Delta t}} + \frac{\Delta t^2}{2\Delta t} \nabla\varphi(\mathbf{y}(t)) = -\nabla\varphi(\mathbf{y}(t)). \quad (9)$$

We expand all terms into powers of Δt at the time t then obtain the following modified differential equation

$$\begin{aligned} &(\ddot{\mathbf{y}} + \frac{\Delta t^2}{12}\mathbf{y}^{(4)} + \dots) + \\ &\Omega \times (\dot{\mathbf{y}} + \frac{\Delta t^2}{3}\mathbf{y}^{(3)} + \dots) = -\nabla\varphi(\mathbf{y}). \end{aligned} \quad (10)$$

Multiplying $\dot{\mathbf{y}}^\top$ in the two sides of the formula. Since $\dot{\mathbf{y}}^\top(\Omega \times \dot{\mathbf{y}}) = 0$, we derive

$$\begin{aligned} & \dot{\mathbf{y}}^\top (\ddot{\mathbf{y}} + \frac{\Delta t^2}{12} \mathbf{y}^{(4)} + \dots) + \\ & \dot{\mathbf{y}}^\top \Omega \times (\frac{\Delta t^2}{3} \mathbf{y}^{(3)} + \dots) = -\dot{\mathbf{y}}^\top \nabla \varphi(\mathbf{y}). \end{aligned} \quad (11)$$

The left hand side can be written as the full differential and $\dot{\mathbf{y}}^\top \nabla \varphi(\mathbf{y}(t)) = \frac{d}{dt} \varphi(\mathbf{y}(t))$, so the modified differential equation has a formal invariant, i.e.,

$$\begin{aligned} & \frac{d}{dt} \left(\frac{1}{2} \dot{\mathbf{y}}^\top \dot{\mathbf{y}} + \varphi(\mathbf{y}) + \frac{\Delta t^2}{12} (\dot{\mathbf{y}}^\top \mathbf{y}^{(3)} - \frac{1}{2} \ddot{\mathbf{y}}^\top \ddot{\mathbf{y}} \right. \\ & \left. + 4\dot{\mathbf{y}}^\top (\Omega \times \ddot{\mathbf{y}})) + \dots \right) = 0. \end{aligned} \quad (12)$$

Thus, we obtain a new formal generalized energy $E_h(\mathbf{y}, \dot{\mathbf{y}}) = E(\mathbf{y}, \dot{\mathbf{y}}) + \Delta t^2 E_2(\mathbf{y}, \dot{\mathbf{y}}) + \dots$, which is an invariant. We only consider the numerical integrator $\{(\mathbf{x}_n, \dot{\mathbf{x}}_n)\}$ in a compact set D . In order to estimate the energy error of the integrator ψ_b (and ψ_v) over a long time, we truncate the E_h in N leading terms, and integrate over the time interval $[0, n\Delta t]$,

$$E_h^N(\mathbf{x}_n, \dot{\mathbf{x}}_n) - E_h^N(\mathbf{x}_0, \dot{\mathbf{x}}_0) = n\Delta t \mathcal{O}(\Delta t^N). \quad (13)$$

The right hand side in the formula (13) is a high order infinitesimal quantity, so

$$|E(\mathbf{x}_n, \dot{\mathbf{x}}_n) - E(\mathbf{x}_0, \dot{\mathbf{x}}_0)| \leq C_N \Delta t^2. \quad (14)$$

where C_N is directly dependent on the value of $\dot{\mathbf{y}}^\top \mathbf{y}^{(3)} - \frac{1}{2} \ddot{\mathbf{y}}^\top \ddot{\mathbf{y}} + 4\dot{\mathbf{y}}^\top (\Omega \times \ddot{\mathbf{y}})$ in the compact set D .

For the integrator ψ_v in formula (8), its modified differential equation as follow

$$\begin{aligned} & (\ddot{\mathbf{y}} + \frac{\Delta t^2}{3} \mathbf{y}^{(4)} + \dots) + \\ & \Omega \times (\dot{\mathbf{y}} - \frac{\Delta t^4}{15} \mathbf{y}^{(5)} + \dots) = -\nabla \varphi(\mathbf{y}). \end{aligned} \quad (15)$$

By the same way, we can also obtain the energy error estimation (14) of ψ_v .

4 THE SYMPLECTIC PROPERTY

For any hyperregular Lagrangian $L(\mathbf{x}, \dot{\mathbf{x}})$, the Euler-Lagrange equations are equivalent to Hamilton's equations of motion. In canonical Hamiltonian system, a map $\phi : \mathbf{z}_n \mapsto \mathbf{z}_{n+1}, \mathbf{z} \in \mathbb{R}^{2d}$ is called symplectic if its Jacobian matrix satisfies the symplectic condition,

$$\left(\frac{\partial \phi}{\partial \mathbf{z}_n} \right)^\top J \left(\frac{\partial \phi}{\partial \mathbf{z}_n} \right) = J. \quad (16)$$

The equivalent expression is that the map ϕ preserves a standard symplectic structure $\frac{1}{2} d\mathbf{z}^\top \wedge J d\mathbf{z}$, i.e., $d\mathbf{z}_{n+1}^\top \wedge J d\mathbf{z}_{n+1} = d\mathbf{z}_n^\top \wedge J d\mathbf{z}_n$.

4.1 The symplectic property – the implicit midpoint scheme ψ_m

We discrete the system (4) by the implicit midpoint scheme (5) and rewrite in the form of only variable \mathbf{x} , as follow

$$\begin{aligned} & \frac{\mathbf{x}_{n+1} - 2\mathbf{x}_n + \mathbf{x}_{n-1}}{\Delta t^2} + 2\Omega \times \frac{\mathbf{x}_{n+1} - \mathbf{x}_{n-1}}{2\Delta t} = \\ & -\frac{1}{2} \left(\nabla \varphi \left(\frac{\mathbf{x}_{n+1} + \mathbf{x}_n}{2} \right) + \nabla \varphi \left(\frac{\mathbf{x}_n + \mathbf{x}_{n-1}}{2} \right) \right). \end{aligned} \quad (17)$$

Considering Lagrangian $L(\mathbf{x}, \dot{\mathbf{x}}) = \frac{1}{2} \dot{\mathbf{x}}^2 + \Omega \cdot (\mathbf{r} \times \dot{\mathbf{r}}) - \varphi(\mathbf{x})$ of the corotating coordinate system, we derive the discrete form of $\int_{t_n}^{t_{n+1}} L(\mathbf{x}(t), \dot{\mathbf{x}}(t)) dt$. The action S_h is

$$S_h(\mathbf{x}_0, \dots, \mathbf{x}_N) = \sum_{n=0}^{N-1} L_h(\mathbf{x}_n, \mathbf{x}_{n+1}), \quad (18)$$

where the L_h is discrete Lagrangian. One of differential form can be written as

$$\begin{aligned} & L_h(\mathbf{x}_n, \mathbf{x}_{n+1}) = \frac{1}{2\Delta t} (\mathbf{x}_{n+1} - \mathbf{x}_n)^2 + \\ & \frac{1}{2} \Omega \cdot (\mathbf{r}_n + \mathbf{r}_{n+1}) \times (\mathbf{r}_{n+1} - \mathbf{r}_n) - \Delta t \varphi \left(\frac{\mathbf{x}_n + \mathbf{x}_{n+1}}{2} \right), \end{aligned} \quad (19)$$

the term $\dot{\mathbf{x}}$ is replaced by $(\mathbf{x}_{n+1} - \mathbf{x}_n)/\Delta t$. According to the discrete Hamilton's principle, the discrete Euler-Lagrange equation reads

$$D_2 L_h(\mathbf{x}_{n-1}, \mathbf{x}_n) + D_1 L_h(\mathbf{x}_n, \mathbf{x}_{n+1}) = 0, \quad (20)$$

where D_i is the partial derivative with respect to the i -th argument. The equation of motion governed by the Lagrangian (Eq. 19) is exactly identical with the equation of midpoint scheme (Eq. 17). In addition, the discrete conjugate momenta is defined by

$$\mathbf{p}_n = -D_1 L_h(\mathbf{x}_n, \mathbf{x}_{n+1}). \quad (21)$$

Using Eq. 20, one can obtain $\mathbf{p}_{n+1} = D_2 L_h(\mathbf{x}_n, \mathbf{x}_{n+1})$. A straightforward calculation gives the equation of $d\mathbf{p}_{n+1} \wedge d\mathbf{x}_{n+1} = d\mathbf{p}_n \wedge d\mathbf{x}_n$ (refer to the Theorem 5.1 of Chapter VI in Hairer et al. (2006)). That means the map $(\mathbf{p}_n, \mathbf{x}_n) \mapsto (\mathbf{p}_{n+1}, \mathbf{x}_{n+1})$ is symplectic and integrator ψ_m is variational symplectic.

Further, substituting the relation of $\mathbf{p} = \partial L / \partial \dot{\mathbf{x}} = \mathbf{v} + (-\omega y, \omega x, 0)$, one can easily compute the map of $(\mathbf{v}_n, \mathbf{x}_n) \mapsto (\mathbf{v}_{n+1}, \mathbf{x}_{n+1})$ (refer to the formula (6) in Tu et al. (2016)), which is a K-symplectic integrator. So the ψ_m also implies a K-symplectic integrator

$$\begin{aligned} \mathbf{v}_n &= \frac{\mathbf{x}_{n+1} - \mathbf{x}_n}{\Delta t} - (\mathbf{x}_{n+1} - \mathbf{x}_n) \times \Omega \\ &+ \frac{\Delta t}{2} \nabla \varphi \left(\frac{\mathbf{x}_{n+1} + \mathbf{x}_n}{2} \right), \\ \mathbf{v}_{n+1} &= \frac{\mathbf{x}_{n+1} - \mathbf{x}_n}{\Delta t} + (\mathbf{x}_{n+1} - \mathbf{x}_n) \times \Omega \\ &- \frac{\Delta t}{2} \nabla \varphi \left(\frac{\mathbf{x}_{n+1} + \mathbf{x}_n}{2} \right). \end{aligned} \quad (22)$$

It is well known that the symplectic integrator has the property of near-conservation of energy over long times. The error is estimated by the form (14) relative to the formal energy of the modified equation (Tang 1994).

4.2 The symplectic property – ψ_b

In this subsection, we show that the numerical method ψ_b is also symplectic. By the same way, we choose the discrete Lagrangian L_h as

$$L_h(\mathbf{x}_n, \mathbf{x}_{n+1}) = \frac{1}{2\Delta t}(\mathbf{x}_{n+1} - \mathbf{x}_n)^2 + \frac{1}{2}\Omega \cdot (\mathbf{r}_n + \mathbf{r}_{n+1}) \times (\mathbf{r}_{n+1} - \mathbf{r}_n) - \Delta t\varphi(\mathbf{x}_n). \quad (23)$$

Similarly, we use the Euler-Lagrangian equation and obtain the discrete equation of

$$D_2 L_h(\mathbf{x}_{n-1}, \mathbf{x}_n) + D_1 L_h(\mathbf{x}_n, \mathbf{x}_{n+1}) = 0, \quad (24)$$

$$\begin{aligned} \mathbf{p}_n &= -D_1 L_h(\mathbf{x}_n, \mathbf{x}_{n+1}), \\ \mathbf{p}_{n+1} &= D_2 L_h(\mathbf{x}_n, \mathbf{x}_{n+1}). \end{aligned} \quad (25)$$

The corresponding equation of motion has the Boris form of

$$\begin{aligned} &\frac{\mathbf{x}_{n+1} - 2\mathbf{x}_n + \mathbf{x}_{n-1}}{\Delta t} + \\ &2\Omega \times \frac{\mathbf{x}_{n+1} - \mathbf{x}_{n-1}}{2} = -\Delta t \nabla \varphi(\mathbf{x}_n). \end{aligned} \quad (26)$$

It proves that the integrator ψ_b is symplectic and defines a symplectic map $(\mathbf{p}_n, \mathbf{x}_n) \mapsto (\mathbf{p}_{n+1}, \mathbf{x}_{n+1})$. Considering the map $(\mathbf{v}_n, \mathbf{x}_n) \mapsto (\mathbf{v}_{n+1}, \mathbf{x}_{n+1})$, one can substitute the relation $\mathbf{p} = \partial L / \partial \dot{\mathbf{x}} = \mathbf{v} + (-\omega y, \omega x, 0)$ and derive a K-symplectic numerical integrator as

$$\begin{aligned} \mathbf{v}_n &= \frac{\mathbf{x}_{n+1} - \mathbf{x}_n}{\Delta t} - (\mathbf{x}_{n+1} - \mathbf{x}_n) \times \Omega \\ &\quad + \Delta t \nabla \varphi(\mathbf{x}_n), \\ \mathbf{v}_{n+1} &= \frac{\mathbf{x}_{n+1} - \mathbf{x}_n}{\Delta t} + (\mathbf{x}_{n+1} - \mathbf{x}_n) \times \Omega. \end{aligned} \quad (27)$$

5 NUMERICAL EXPERIMENTS

In this section, we numerically present the behaviors of the integrators ψ_b , ψ_v and ψ_m in two kinds of extreme potential energy, a extensive Quadratic potential and restricted three-body Earth-Moon system. The reference orbits are computed by RK3 (third-order Runge-Kutta method). Specifically, the form of RK3 reads

$$\begin{cases} \mathbf{z}_{n+1} = \mathbf{z}_n + \frac{\Delta t}{2} [f(K_1) + f(K_2)], \\ K_1 = \mathbf{z}_n + \frac{\Delta t}{6} [3f(K_1) - \sqrt{3}f(K_2)], \\ K_2 = \mathbf{z}_n + \frac{\Delta t}{6} [\sqrt{3}f(K_1) + 3f(K_2)]. \end{cases} \quad (28)$$

5.1 Quadratic potential

We consider a homogeneous rotating top-hat density sphere with the quadratic potential of $U(\mathbf{x}) = 4(x^2 + y^2 + z^2)$. We set the rotating speed $\omega = \pi/40$ and the period is 80. The initial position and velocity is $\mathbf{x} = (-1.9, 0, 0)$ and $\mathbf{v} = (0, -1.0, 0)$, respectively. The time step is fixed to $\Delta t = 0.02$.

In panel (a) of Fig. 1, we find that the numerical integrators ψ_b, ψ_v , the midpoint scheme ψ_m , and RK3 all give the accurate orbit in the first rotation period. In panel (b) of Fig. 1, ψ_b, ψ_v , the midpoint scheme ψ_m provide the correct orbit in the 300th rotation period while RK3 fails. Relative errors of the energy $(E(n\Delta t) - E_0)/E_0$ of the numerical methods ψ_b, ψ_v and the implicit midpoint scheme ψ_m are bounded, which is shown in Fig. 2. In particular, the energy E is a quadratic invariant along the flow of phase space. The implicit midpoint scheme ψ_m preserve the energy E exact. So the relative energy error $(E(n\Delta t) - E_0)/E_0$ of the implicit midpoint scheme ψ_m is tiny. These numerical results verified the properties of long-term near-conservation of energy for ψ_b, ψ_v , and the midpoint scheme ψ_m and demonstrate the property of symplecticity of ψ_b, ψ_m . Since RK3 have not such good properties, it is not surprising on the failure of RK3 in orbit scale and energy conservation.

5.2 Earth-Moon system

The motion in the corotating coordinate is critical in the field of astronomy and space science. In the design of spacecraft orbit, the earth and moon disturbances should be taken into account when calculating the orbits of satellites near the earth and moon. In this case, the motions of the earth, moon and satellite form a restricted three body problem, which is a kind of corotating coordinate system.

The restricted three-body problem can be written in the form of (3) with potential

$$\begin{aligned} U(\mathbf{x}) &= -\frac{GM_1}{\sqrt{(x-x_1)^2 + (y-y_1)^2 + z^2}} \\ &\quad -\frac{GM_2}{\sqrt{(x-x_2)^2 + (y-y_2)^2 + z^2}}, \end{aligned} \quad (29)$$

which has been widely studied (Gao & Zhang 2014; Perdomo 2017; Abouelmagd et al. 2020). We expand into the component form of (x, y, z) , as follow

$$\begin{aligned} \frac{d^2 x}{dt^2} - x\omega^2 - 2\omega \frac{dy}{dt} &= -\frac{GM_1(x-x_1)}{R_1^3} - \frac{GM_2(x-x_2)}{R_2^3}, \\ \frac{d^2 y}{dt^2} - y\omega^2 + 2\omega \frac{dx}{dt} &= -\frac{GM_1(y-y_1)}{R_1^3} - \frac{GM_2(y-y_2)}{R_2^3}, \\ \frac{d^2 z}{dt^2} &= -\frac{GM_1 z}{R_1^3} - \frac{GM_2 z}{R_2^3}, \end{aligned}$$

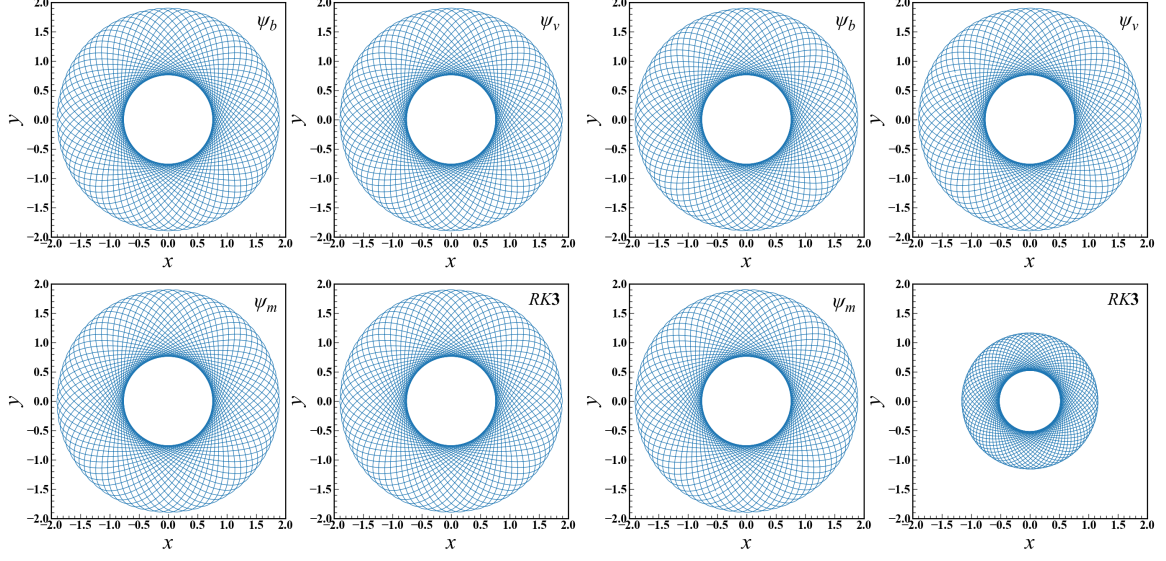


Fig. 1 The orbits are given by ψ_b , ψ_v , the midpoint scheme ψ_m and RK3 in the first rotation period (left) and the 300th rotation period (right).

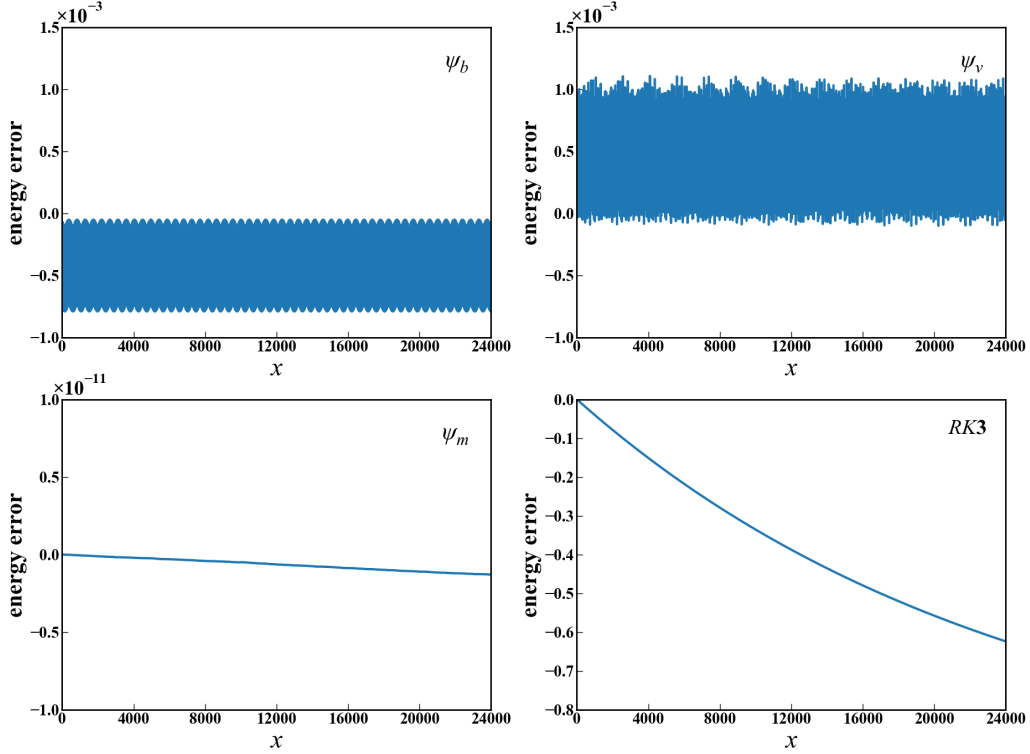


Fig. 2 Relative errors of the energy $(E(n\Delta t) - E_0)/E_0$ are given by ψ_b , ψ_v , the midpoint scheme ψ_m , and RK3 over the time interval $[0, 24000]$.

where $R_1 = ((x - x_1)^2 + (y - y_1)^2 + z^2)^{1/2}$, $R_2 = ((x - x_2)^2 + (y - y_2)^2 + z^2)^{1/2}$ and the coordinate origin is mass center of the system.

We study the Earth-Moon system. The unit of distance is an Astronomical Unit (1.4959787e13 cm), time unit is an earth day (86400 second) and mass unit is kilo-

gram. The corresponding normalized parameters $GM_1 = 0.8997011603631609\text{e-}09$ (following the parameters in (Tu et al. 2020)), $GM_2 = 0.0123GM_1$, the distance of between earth and moon $R = 2.56267\text{e-}3$, $r_1 = -M_2R/(M_1 + M_2)$, $r_2 = M_1R/(M_1 + M_2)$ and the rotation speed $\omega = \sqrt{G(M_1 + M_2)/R^3}$. The earth initial

position is $(x_1, y_1) = (r_1, 0)$ and the moon initial position $(x_2, y_2) = (r_2, 0)$. We set two groups of initial conditions to check the behaviors of the above numerical integrators.

Orbit 1: we set initial position of a massless object at $\mathbf{x} = (-r_2/4, 0, 0)$, velocity $\dot{\mathbf{x}} = (0, 1.69561e-3, 0)$ and step-size $\Delta t = 0.01$. The orbit of the celestial object is numerically integrated over the time interval of $[0, 40000]$. The energy of the system is a conserved quantity, $E_0 = -7.1941456034028234e - 8$.

Orbit 2: we set initial position $\mathbf{x} = (-3r_2/5, 0, 0)$, velocity $\dot{\mathbf{x}} = (0, 1.35057e-3, 0)$ and step-size $\Delta t = 0.04$. The orbit is integrated during time $t \in [0, 10^5]$. The energy of the system is $E_0 = 2.4213436261924679e - 7$.

In Fig. 3, we find that the numerical integrator ψ_b and ψ_m give the correct orbits over long time, but ψ_v and RK3 fail. Fig. 4 and Fig. 5 present that the relative energy error $(E(n\Delta t) - E_0)/E_0$ with respect to the initial values of two orbits, respectively. In both case, ψ_b and ψ_m perserve near-conservation of energy over long time, due to symplectic. In contrast, the error of ψ_v and RK3 diverge. Note that non-symplectic ψ_v actually maintains the property of near-conservation of energy, but it still behaves bad.

Besides the conservation of energy, we check the phase-drifting of the orbits for ψ_b and ψ_m . Fig. 6 shows numerical solutions of the 20-th and 100-th orbit period in the x-direction with respect to the initial values of two orbits, respectively. The ψ_m^{10} denotes a 10th order composition method (formula (17) in Sofroniou & Spaletta (2005)) of midpoint scheme and we uses 10 times finer step-size than the ψ_b and ψ_m .

Comparing with the integrator ψ_m , we find that the phase of ψ_b and ψ_m are consistent with the high-order method ψ_m^{10} and ψ_b is slightly better than ψ_m . A reasonable speculation is that the integrator ψ_b is explicit and there is less rounding error accumulation from the iterations than an implicit ψ_m .

6 CONCLUSION

In this paper, we investigated the symplectic property of three integrators, ψ_b , ψ_v and ψ_m in corotating coordinates. All of them are near-conservation of energy for long-term evolution and ψ_b and ψ_m are proved as symplectic schemes. In particular, the integrators of ψ_b and ψ_m are variational symplectic by directly discretizing the motion equation and non-canonical Hamiltonian system, respectively.

Two groups of numerical experiments, rotating quadratic potential and earth-moon system, are carried out to verify our theoretical analysis. The energy error of ψ_b and ψ_m is indeed bounded and the phase shift also behaves well. However, the scheme ψ_v is theoretically a conservative scheme, but it fails in phase-space evolution.

Acknowledgements We acknowledge the support from National SKA Program of China (Grant No. 2020SKA0110401), National Natural Science Foundation of China (Grant No. 11988101, 12171466), Special Research Assistant Program of the Chinese Academy of Sciences and K.C.Wong Education Foundation.

References

- Abouelmagd, E. I., García Guirao, J. L., & Pal, A. K. 2020, *New Astronomy*, 75, 101319
- Akiyama, Y., Bando, M., & Hokamoto, S. 2019, *Acta Astronautica*, 160, 672
- Binney, J., & Tremaine, S. 2008, *Galactic Dynamics: Second Edition*
- Boris, J. 1970, *Relativistic plasma simulation-optimization of a hybrid code*, 3
- Candy, J., & Rozmus, W. 1991, *Journal of Computational Physics*, 92, 230
- Channell, P. J., & Scovel, C. 1990, *Nonlinearity*, 3, 231
- Ellison, C. L., Burby, J. W., & Qin, H. 2015, *Journal of Computational Physics*, 301, 489
- Feng, K. 1985, in *Proceedings of 1984 Beijing Symposium on Differential Geometry and Differential Equations*, edited by K. Feng (Science Press, Beijing), 42
- Feng, K. 1986, *Journal of Computational Mathematics*, 4, 279
- Forest, E., & Ruth, R. D. 1990, *Physica D: Nonlinear Phenomena*, 43, 105
- Gao, F. B., & Zhang, W. 2014, *AJ*, 148, 116
- Hairer, E., & Lubich, C. 2018, *BIT Numerical Mathematics*, 301, 969
- Hairer, E., Lubich, C., & Wanner, G. 2006, *Geometric Numerical Integration. Structure-Preserving Algorithms for Ordinary Differential Equations*, 2nd edn. (Berlin: Springer), iD: unige:12343
- Oshima, K., & Yanao, T. 2019, *Celestial Mechanics and Dynamical Astronomy*, 131, 23
- Perdomo, O. 2017, *Celestial Mechanics and Dynamical Astronomy*, 129, 89
- Qin, H., Zhang, S., Xiao, J., et al. 2013, *Physics of Plasmas*, 20, 084503
- Sofroniou, M., & Spaletta, G. 2005, *Optimization Methods and Software*, 20, 597
- Tang, Y.-F. 1994, *Computers & Mathematics with Applications*, 27, 31
- Tu, X., Murua, A., & Tang, Y. 2020, *BIT Numerical Mathematics*, 129, 509
- Tu, X., Zhu, B., Tang, Y., et al. 2016, *Physics of Plasmas*, 23, 122514

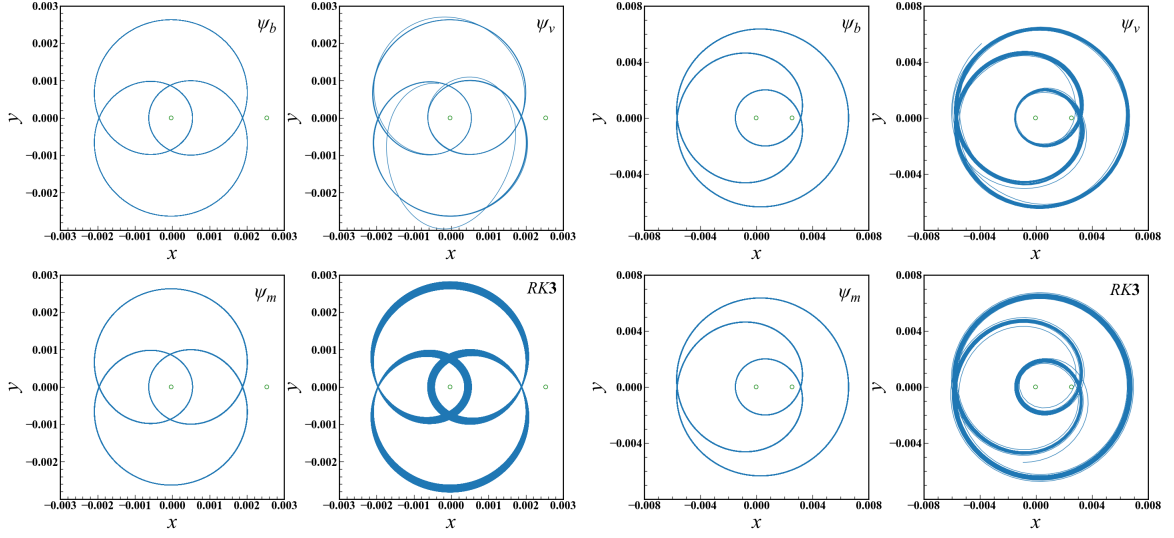


Fig. 3 Numerical orbits are given by ψ_b , ψ_v , ψ_m and RK3 of orbit 1 (left) and orbit 2 (right), respectively.

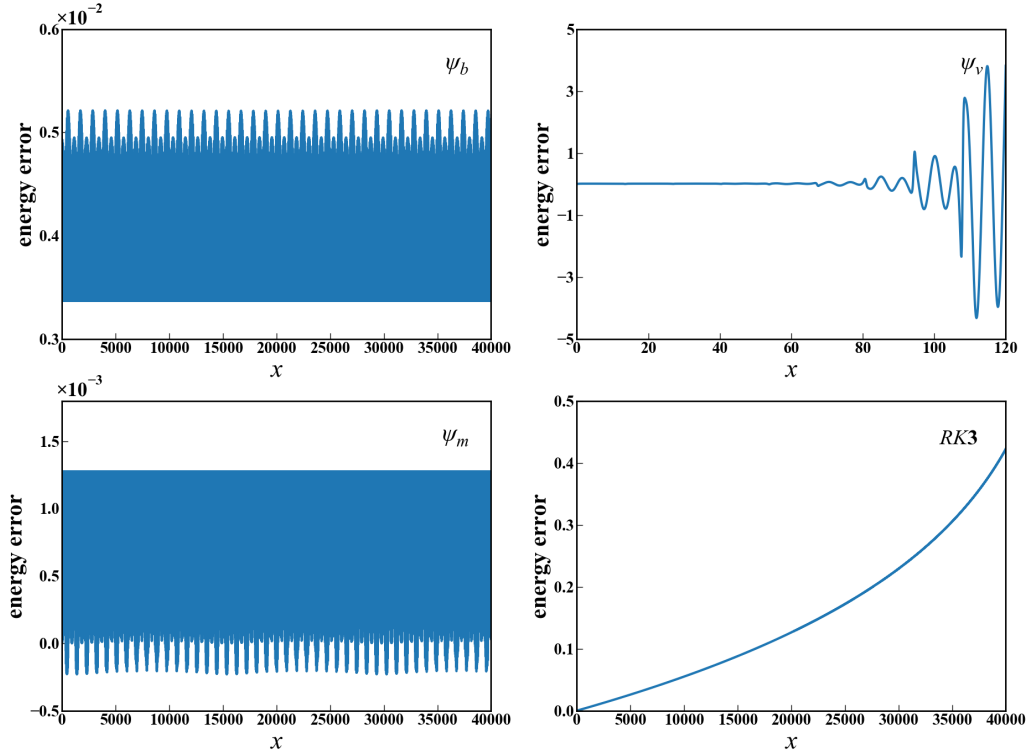


Fig. 4 Relative errors of the energy $(E(n\Delta t) - E_0)/E_0$ are given by ψ_b , ψ_v , ψ_m , and RK3 of orbit 1 over the time interval $[0, 40000]$.

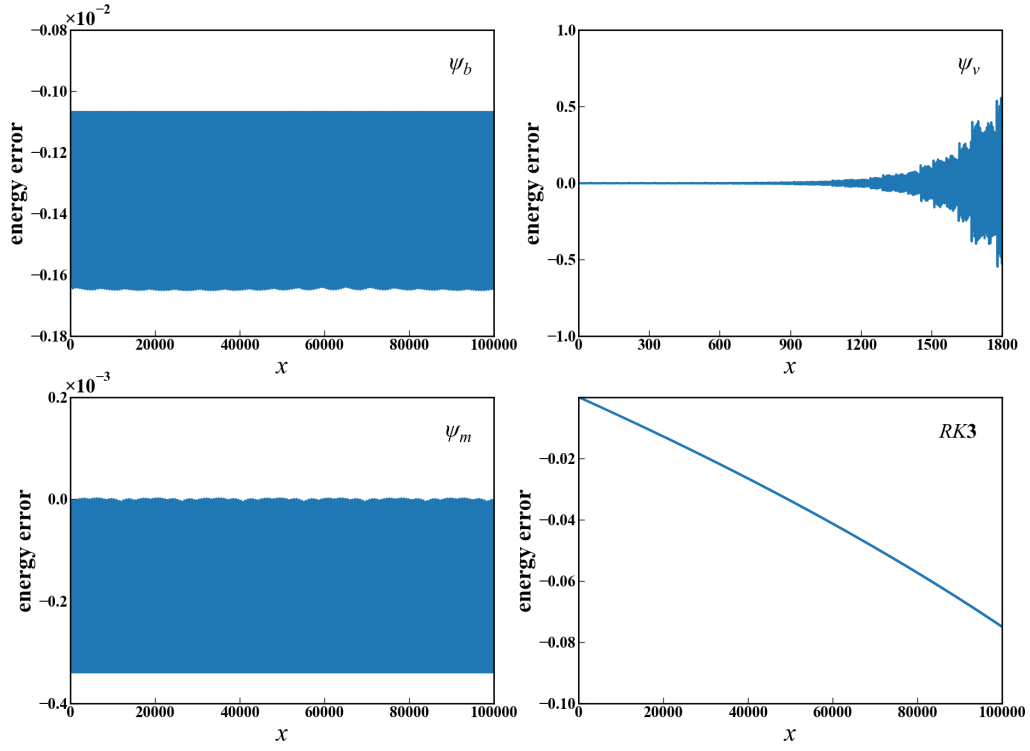


Fig. 5 Relative errors of the energy $(E(n\Delta t) - E_0)/E_0$ are given by ψ_b, ψ_v, ψ_m , and RK3 of orbit 2 over the time interval $[0, 10^5]$.

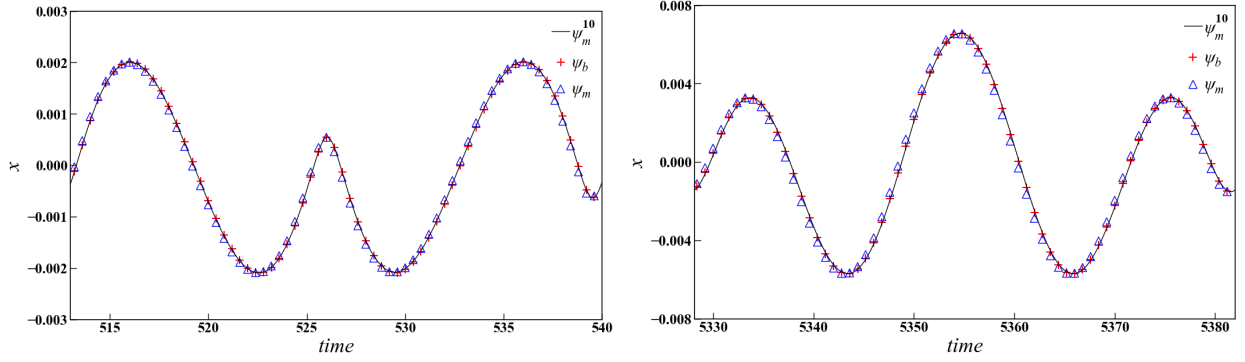


Fig. 6 Numerical solutions in the x -direction of orbit 1 in the 20th orbit period (the left panel) and orbit 2 in the 100th orbit period (the right panel).